Interactions between hepatic glucose and fat metabolism in animal models of insulin resistance

Wiegman, Cornelis Harm

Chapter 4

Hepatic VLDL production in ob/ob mice is not stimulated by massive *de novo* lipogenesis and is less sensitive to the suppressive effects of insulin

Coen H. Wiegman[1], Robert H.J. Bandsma[1], Margriet Ouwens[2], Fjodor H. van der Sluijs[1], Rick Havinga[1], Theo Boer[1], Dirk-Jan Reijngoud[1], Johannes A. Romijn[3], and Folkert Kuipers[1]

Submitted

[1] Department of Pediatrics, Academic Hospital Groningen, Groningen, The Netherlands

[2] From the Department of Molecular Cell Biology, Academic Hospital Leiden, Leiden, The Netherlands

[3] From the Department of Endocrinology, Academic Hospital Leiden, Leiden

ABSTRACT

Type 2 diabetes mellitus in humans is associated with increased *de novo* lipogenesis (DNL), increased fatty acid (FA)-flux from peripheral tissues, decreased FA oxidation and hepatic steatosis. In type 2 diabetes mellitus, production of VLDL is increased and resistant to the suppressive effects of insulin. The relationships between FA metabolism, hepatic steatosis and VLDL production are incompletely understood. We investigated VLDL formation in relation to DNL and insulin sensitivity in female ob/ob mice, a model of type 2 diabetes with hepatic steatosis. Hepatic triglyceride (5-fold) and cholesteryl ester (15-fold) contents were increased in ob/ob mice compared to lean controls. Hepatic DNL was increased ~10-fold in ob/ob mice whereas hepatic cholesterol synthesis was not affected. Basal rates of hepatic VLDL-triglyceride and -apoB100 production were also similar between the groups. Hyperinsulinemic clamping reduced VLDL-triglyceride and -apoB100 production rate by ~60% and ~75%, respectively, in lean mice but only by ~20% and ~20%, respectively, in ob/ob mice. No difference in hepatic expression of genes encoding apolipoprotein B, microsomal triglyceride transfer protein and diacylglycerolacyltransferase-1 were found. Hepatic gene expression and protein phosphorylation of the insulin receptor and insulin receptor substrate-isoforms were reduced in ob/ob mice. Thus, strongly induced hepatic DNL is not associated with increased basal VLDL production in ob/ob mice, which might be related to differential hepatic zonation of apoB synthesis (periportal) and lipid accumulation (perivenous) and/or relatively low rates of cholesterogenesis. Insulin is unable to effectively suppress VLDL-triglyceride production in ob/ob mice, presumably due to impaired insulin signaling.

INTRODUCTION

Type 2 diabetes mellitus (DM2) is associated with increased *de novo* lipogenesis (DNL), decreased plasma fatty acid (FA) oxidation and an increased FA-flux from peripheral tissues to the liver (1). These factors may all contribute to hepatic steatosis and increased hepatic VLDL production, two characteristic hallmarks of type 2 diabetes (2), and are probably related to insulin resistance. The relative contribution of the various pathways in hepatic lipid metabolism to the development of a fatty liver and disturbances in VLDL production is unknown but may, at least in part, be related to the localization of these processes within the liver. Fatty acid synthesis and TG accumulation occur predominantly in the perivenous areas (zone 3) of the liver whereas FA oxidation is more associated with the periportal areas (zone 1) of the liver (3,4). VLDL secretion has not been restricted to a specific hepatic zone: zonation of apoB gene expression and/or synthesis has not been reported.

Leptin-deficient ob/ob mice develop a fatty liver, insulin resistance and hyperlipidemia (5-7). The contribution of hepatic lipoprotein production to the development of hyperlipidemia in these mice is not clear. Hyperglycemia together with an increased glycolytic activity in ob/ob mice may lead to an increased availability of acetylCoA residues for DNL (8). The high glycolytic rate in these mice is reflected by increased expression levels and activities of enzymes involved in this metabolic pathway, i.e., glucokinase (9,10), phosphofructokinase (8) and pyruvate kinase (8,9). Furthermore, elevated plasma FFA levels (10) together with increased hepatic expression of fatty acid translocase (FAT or CD36) and plasma membrane-fatty acid binding protein (pmFABP) have been reported in this model (11). Increased endoplasmic reticulum (ER)-associated acetylCoA synthase (ACS) activity may increase the FA availability for esterification rather than for oxidation (11), which could contribute in increased TG and cholesteryl ester deposition and/or incorporation into VLDL.

Hepatic insulin resistance seen in DM2 is associated with increased VLDL production (2). Acute hyperinsulinemia reduces VLDL production in healthy volunteers (12-14) but not in DM2 patients (2) and obese individuals (13). Despite the insulin resistant condition and an increased hepatic TG content in ob/ob mice, a decreased VLDL-TG production rate under basal fasted conditions has been reported in this model (15,16). However, increased VLDL-TG secretion in ob/ob mice associated with enhanced expression and activity of the microsomal triglyceride transfer protein (MTP) has also been reported (17). The reason for these discrepant observations is unknown. The impact of insulin on VLDL production in the ob/ob mouse model has not been reported previously. Therefore, we quantified hepatic DNL and cholesterol synthesis using mass isotopomer distribution analysis (MIDA) and related the synthesis rates to VLDL-TG and -apoB100 production rates determined under basal conditions and during hyperinsulinemic clamp conditions in ob/ob mice and in lean littermates. Hepatic insulin signaling and expression levels of genes encoding transcription factors and important enzymes involved in fatty acid and cholesterol metabolism, VLDL formation and insulin signaling, were studied to provide a mechanistic basis for our findings.

MATERIAL AND METHODS

Animals. Female ob/ob and lean littermates were purchased from Harlan (Zeist, The Netherlands) and housed in a light- and temperature controlled facility. Experimental protocols were approved by the local Experimental Ethical Committee for Animal Experiments.

Analytical kits. Plasma and hepatic TG, cholesterol and glucose levels were determined by commercially available kits (Roche, Mannheim, Germany). Plasma and hepatic phospholipid concentrations and plasma FFA concentrations were determined with Phospholipid-kit and NEFA-C kit, respectively (Wako Chemical GmbH, Neuss, Germany). Plasma insulin was determined by a radio-immunoassay (RIA) RI-13K (Linco Research, Inc., St. Charles).

Experimental procedures. Female ob/ob (n=5) and lean mice (n=5), weighing between 51-63 gram and 24-28 gram respectively, were fed normal chow diet (RMH-B 2181, Hope Farms BV, Woerden, The Netherlands) enriched with 2% [1-^{13}C]-acetate (Isotec, Miamisburg, OH), which was given *ad libitum*. After 11 days mice were fasted for a period of 4 hours. Mice were anaesthetized with halotane and the liver was excised. A portion of abdominal fat was also collected. Liver and fat tissue were immediately frozen in liquid nitrogen and stored at -80ºC. Blood was isolated by heart puncture and immediately placed on ice in EDTA containing tubes and centrifuged 10 minutes at 5,000 rpm at 4ºC. Plasma was stored at -20ºC until analysis.

Hyperinsulinemic clamp. To study the effects of insulin on lipoprotein metabolism a second groups of lean and ob/ob mice received a hyperinsulinemic clamp or a saline infusion (n=4/group) under anesthesia. Based on euglycemic insulin clamps performed in rats and mice by Hawkins and Rossetti *et al.* (18,19) where insulin concentrations were fixed at ~25 ng/ml we used a single infusate containing all constituents, aimed to result in hyperinsulinemia and euglycemia. The procedure was tested in pilot experiments. The infusate contained insulin (18 mU/kg/min; Novo Nordisk, Bagsvaerd, Denmark), somatostatin (1.5 μg/kg/min; UCB, Breda, The Netherlands) to suppress the endogenous insulin production, and glucose (25 mg/kg/hr; Merck, Darmstadt, Germany) to maintain normal plasma glucose concentration. All components were freshly prepared in saline containing 1.5% BSA (Sigma, St. Louis, MO). Plasma glucose concentration was determined with a GlucoTouch-glucose analyzer (LifeScan, Beerse, Belgium). The total infusion time was 2 hours. After 1 hour mice received a Triton WR1339 infusion (Tyloxpol; Sigma, St. Louis, MO) 12% $^{wt}/_{wt}$ solution dissolved in saline, dose 5 ml/kg lean BW. Triton blocks the lipolysis of secreted lipoprotein particles, therefore, the accumulation of these lipoprotein particles in time allows us to calculate production rates (20). After injection blood samples were taken after 30 and 60 minutes. At the end of the experiment a 200 μl plasma sample was obtained by heart puncture to isolate VLDL particles. VLDL production rates were calculated from the slope of the linear-TG-accumulation-curves in time. Particles were isolated using a solution of 15.3% NaCl and 35.4% KBr (final concentration 0.65% and 1.52%, respectively) in saline with a density <1.019 g/ml. Plasma (0.2 ml) was used with 0.8 ml of the NaCl-KBr solution and centrifuged for 100 minutes at 120,000 rpm and 4ºC. Tubes were sliced at 1.5 cm from top and the top-fraction, containing the VLDL-particles, was collected and frozen at -80ºC until composition analysis and apoB quantification. VLDL particle size was determined in isolated VLDL fractions using a Submicron Particle Sizer, (Autodilute, model 370; Nicomp, Santa Barbara, CA, US).

Liver lipid analysis. Liver lipids were extracted following a modified Bligh & Dyer method (21) and determined by commercially available kits. Total protein of tissue homogenates was determined using the method described by Lowry *et al.* (22).

Histology. To study the localization of hepatic TG accumulation and VLDL production, liver morphology, neutral lipids and apolipoprotein B (apoB) mRNA were visualized as indicators

for TG deposition and VLDL formation, respectively. Hepatic morphology was visualized by standard Hematoxilin Eosin (HE)-staining and neutral lipids were visualized by "Oil-Red-O" (ORO) staining. ApoB *in situ* hybridization technique was described previously for apoE (23). The pGEM-3z vector in which apoB cDNA was placed was a gift form dr. H.M. Prinsen (TNO, Leiden).

Mass isotopomer distribution analysis. The MIDA technique allows measuring the biosynthesis of polymers *in vivo* and is described in great detail elsewhere (24,25). Briefly, the relative abundance of different mass isotopomers during feeding of a [1-^{13}C]-acetate-enriched diet was determined. The enrichment of the pool of acetylCoA precursor units (p) that has entered newly synthesized cholesterol and palmitate can be calculated by comparing it with a theoretical table generated using binomial expansion and known isotope frequencies of the atomic isotopes. When the enrichment of the acetylCoA pool is known it becomes possible to calculate the fraction (f) of newly synthesized cholesterol and palmitate molecules in liver and adipose tissue homogenates. To determine the absolute amount of newly synthesized hepatic cholesterol and palmitate we multiplied f by the total amount of hepatic free cholesterol and palmitate, respectively.

Gas chromatography/mass spectrometry (GC/MS) analysis. Plasma cholesterol was extracted and derivatized as described elsewhere (26). Palmitate from plasma and liver samples were trans-methylated according to Lepage *et al.* (27). Cholesterol and fatty acid derivates were analyzed on a magnetic sector mass spectrometer (70-250S; VG, Manchester, U.K.) using a Chrompack CP-Sil 19 column (Middelburg, the Netherlands) for assessment of isotopomer distribution patterns. For cholesterol samples, the oven temperature increased from 120 to 260ºC at a rate of 20ºC/min, from 260 to 280ºC at 2.5ºC/min and finally from 280 to 300ºC at 20ºC/min. The ions at m/z 368 to 371 were measured under selected ion recording. For FA samples the oven temperature increased from 100 to 300ºC at a rate of 12.5ºC/min. The ions of the palmitate derivative were measured at m/z 270 to 272 under selected ion recording. FA methyl esters were separated and quantified by gas liquid chromatography as earlier described (28) using heptadecanoic acid (17:0) as internal standard.

ApoB quantification. ApoB100 concentrations were quantified with a reference to an IDL apoB100 standard isolated from healthy human subjects (29). Since human liver does not produce ApoB48 containing lipoprotein particles we were not able to quantify apoB48 levels. Isolated VLDL samples (10 µl) were delipidated with methanol and diethylether and dried under nitrogen. Delipidated lipoproteins were reduced in SDS sample buffer (8 M urea, 10 mM Tris base, 2% SDS, 10% glycerol, 5% β-mercaptoethanol) and separated by SDS-PAGE using 4-15% gradient gels (Ready gels, Biorad, Hercules, CA) at 100 V for 30 minutes followed by 120 V for 120 minutes. Gels were either stained with a silver-staining procedure (29) or were prepared for Western blot analysis. Proteins were transferred on nitrocellulose membranes (Hybond ECL, Amersham Pharmacia Biotech, Buckinghamshire, UK) by Western blotting for 120 minutes at 250 mA. Blots were put on skimmed milk over night and stained with the primary polyclonal antibody against human apolipoprotein B, raised in sheep (dilution 1:100,000; Roche, Mannheim, Germany) and secondary IgG, anti-sheep antibody conjugated with horseradish-peroxidase activity (dilution 1:10,000; Calbiochem, San Diego, CA). ECL activation of the peroxidase was detected on film. ApoB100 levels were quantified with a reference to an IDL apoB100 standard isolated from healthy human subjects.

Table 1. List of sequences of primers and probes used.

Standard	Type	Sequence	Gen-Bank no.
β-*Actin*	forward	AGC CAT GTA CGT AGC CAT CCA	NM_007393
	reverse	TCT CCG GAG TCC ATC ACA ATG	
	probe	TGT CCC TGT ATG CCT CTG GTC GTA CCAC	
Transcription factors			
Srebp-1c	forward	GGA GCC ATG GAT TGC ACA TT	BI656094
	reverse	CCT GTC TCA CCC CCA GCA TA	
	probe	CAG CTC ATC AAC AAC CAA GAC AGT GAC TTC C	
Srebp-2	forward	CTG CAG CCT CAA GTG CAA AG	AF374267
	reverse	CAG TGT GCC ATT GGC TGT CT	
	probe	CCA TCC AGC AGC AGG TGC AGA CG	
Pparα	forward	TAT TCG GCT GAA GCT GGT GTA C	X57638
	reverse	CTG GCA TTT GTT CCG GTT CT	
	probe	CTG AAT CTT GCA GCT CCG ATC ACA CTT G	
Pparγ	forward	CAC AAT GCC ATC AGG TTT GG	NM_011146
	reverse	GCT GGT CGA TAT CAC TGG AGA TC	
	probe	CCA ACA GCT TCT CCT TCT CGG CCT G	
Lxr	forward	GCT CTG CTC ATT GCC ATC AG	AF085745
	reverse	TGT TGC AGC CTC TCT ACT TGG A	
	probe	TCT GCA GAC CGG CCC AAC GTG	
Chrebp	forward	GAT GGT GCG AAC AGC TCT TCT	AF156604
	reverse	CTG GGC TGT GTC ATG GTG AA	
	probe	CCA GGC TCC TCC TCG GAG CCC	
DNL, cholesterogenisis and β-oxidation			
Fas	forward	GGC ATC ATT GGG CAC TCC TT	AF127033
	reverse	GCT GCA AGC ACA GCC TCT CT	
	probe	CCA TCT GCA TAG CCA CAG GCA ACC TC	
Acc	forward	GCC ATT GGT ATT GGG GCT TAC	AF374170
	reverse	CCC GAC CAA GGA CTT TGT TG	
	probe	CTC AAC CTG GAT GGT TCT TTG TCC CAG C	
Hmgr	forward	CCG GCA ACA ACA AGA TCT GTG	BB664708
	reverse	ATG TAC AGG ATG GCG ATG CA	
	probe	TGT CGC TGC TCA GCA CGT CCT CTT C	
Cpt1a	forward	CTC AGT GGG AGC GAC TCT TCA	AF 017175
	reverse	GGC CTC TGT GGT ACA CGA CAA	
	probe	CCT GGG GAG GAG ACA GAC ACC ATC CAA C	
Mcad	forward	GCA GCC AAT GAT GTG TGC TTA C	NM_007382
	reverse	CAC CCT TCT TCT CTG CTT TGG T	
	probe	CCC TCC GCA GGC TCT GAT GTG G	
Hmgs	forward	TGG TGG ATG GGA AGC TGT CTA	U12790
	reverse	TTC TTG CGG TAG GCT GCA TAG	
	probe	CCA AGG CCC GCA GGT AGC ACT G	
VLDL metabolism			
Apob	forward	GCC CAT TGT GGA CAA GTT GAT C	AW012827
	reverse	CCA GGA CTT GGA GGT CTT GGA	
	probe	AAG CCA GGG CCT ATC TCC GCA TCC	
Apobec-1	forward	TCG TCC GAA CAC CAG ATG CT	NM_031159
	reverse	GGT GTC GGC TCA GAA ACT CTG T	
	probe	CCT GGT TCC TGT CCT GGA GTC CCT G	
Apoe	forward	CCT GAA CCG CTT CTG GGA TT	NM_009696
	reverse	GCT CTT CCT GGA CCT GGT CA	
	probe	AAA GCG TCT GCA CCC AGC GCA GG	
Dgat-1	forward	GGT GCC GTG ACA GAG CAG AT	NM_010046
	reverse	CAG TAA GGC CAC AGC TGC TG	
	probe	CTG CTG CTA CAT GTG GTT AAC CTG GCC A	
Mttp	forward	CAA GCT CAC GTA CTC CAC TGA AG	NM_008642
	reverse	TCA TCA TCA CCA TCA GGA TTC CT	
	probe	ACG GCA AGA CAG CGT GGG CTA CA	
Insulin signaling			
Ir	forward	TGA GTC AGC CAG TCT TCG AGA A	NM_010568
	reverse	ACT ACC AGC ATT GGC TGT CCT T	
	probe	CTG CCA TCA TGT GGT CCH CCT TCT	
Irs-1	forward	AGC ACC TGG TGG CTC TCT ACA	NM_010570
	reverse	CAG CTG CAG AAG AGC CTG GTA	
	probe	CTC GCT ATC CGC GGC AAT GGC	
Irs-2	forward	AGT CCC ACA TCG GGC TTG AAG	AF090738
	reverse	GGT CTG CAC GGA TGA CCT TAG	
	probe	CCT TCA AGT CAG CCA GCC CCC TG	

Hepatic gene expression. Hepatic gene expression levels were quantified by real time polymerase chain reaction (PCR) analysis during basal conditions and hyperinsulinemia. Total RNA was isolated from approximately 30 mg of liver tissue using Trizol-method (GIBCO, Paisley, UK) followed by the SV Total RNA Isolation System (Promega, Madison, WI) according to the protocols provided by the manufacturer. Isolated total RNA was converted to single stranded cDNA by a reverse transcription procedure with M-Mulv-RT (Boehringer Mannheim, Mannheim, Germany) according to manufacture's protocol. cDNA levels were measured by real-time PCR using the ABI Prism 7700 Sequence Detection System (Applied Biosystems, Foster City, CA). For the PCR amplification studies, an amount of cDNA corresponding to 10 ng of total RNA was amplified using the qPCR core kit (Eurogentec, Seraing, Belgium). Procedures were essentially according to manufacturer's protocol and optimised for amplification of the particular gene using the appropriate forward

and reverse primers (GIBCO, Paisley, UK) and a template specific 3'-TAMRA, 5'-6-FAM labeled Double Dye Oligonucleotide probe (Eurogentec, Seraing, Belgium). In the same experiments, calibration curves were run on serial dilutions of a 8x concentrated cDNA solution as used in the assay, resulting in a series containing 8x, 4x, 2x, 1x, 0.5x, 0.125x, 0.062x, and 0.031x of the cDNA present in the assay incubation. Both assay and calibration incubations were done simultaneously. During the amplification, the breakdown of the probe releases the fluorescent 6-FAM-dye, resulting in an increase in fluorescence. The fluorescence data obtained were processed using the software program ABI Sequence Detector v1.6.3 (System Applied Biosystems, Foster City, CA). All quantified expression levels were within the linear part of the calibration curves and calculated using these curves. The primers and probe sets used are listed in Table 1. The relative intensity of the product bands was determined by a CCD video camera of the ImageMaster VDS system (Pharmacia, Upsalla, Sweden) and quantified by Image software.

Hepatic insulin signaling. For analysis of IRβ and IRS-1,2,3 phosphorylation, liver parts were homogenized in RIPA-buffer (30 mM Tris, pH 7.5, 1 mM EDTA, 150 mM NaCl, 0.5% Triton X-100, 0.5% deoxycholate, 1 mM sodium orthovanadate, 10 mM sodium fluoride, and protease inhibitors (Complete: Boehringer Mannheim)) using a Ultraturrax mixer. Lysates were cleared by centrifugation (14 krpm; 15 min; 4ºC). Protein content of supernatant were determined using BCA-kit (Pierce, Rockford, IL). A total of 25 μg of protein was analysed by immunoblotting for expression of IRβ subunit (Transduction Laboratories), IRS-1 (30), IRS-2 (31) and IRS-3. Anti- IRS3 antibody was obtained by immunized rabbits with a recombinant His-tagged IRS3 fusion protein produced from pET16B-IRS3 (aa198-494 of rat IRS3) as decribed by Ouwens *et al.* 1994 (30).

Table 2. Plasma and hepatic parameters after a 4 hr fast in lean and ob/ob mice (n=5/group), *p<0.05, Mann-Whitney U.

	lean	ob/ob
Plasma		
Glucose (mM)	8.6±3.0	16.9±4.6*
Insulin (ng/ml)	1.3±0.9	6.9±0.6*
Triglycerides (mM)	0.3±0.03	0.7±0.1*
Cholesterol (mM)	1.7±0.4	4.1±0.3*
Free fatty acids (mM)	0.7±0.1	1.3±0.1*
Liver		
Liver weight (gram)	1.3±0.1	2.7±0.3*
Triglycerides (μmol/liver)	1.5±0.5	7.5±1.1*
Total cholesterol (μmol/liver)	1.7±0.6	4.4±1.1*
Free cholesterol (μmol/liver)	1.7±0.1	2.7±0.5*
Cholesteryl esters (μmol/liver)	0.1±0.01	1.5±0.8*
Phospholipids (μmol/liver)	0.4±0.1	0.6±0.3
Glucose-6-phosphate (μmol/liver)	0.2±0.4	0.3±0.1
Glycogen (μmol/liver)	272±27	501±54*

RESULTS

Animal characteristics. Mean body weight was 26±1 *vs.* 58±5 gr in the lean and ob/ob mice, respectively ($p<0.05$). Fasting plasma glucose, insulin, TG, cholesterol, and FFA concentrations were elevated in ob/ob mice (Table 2). Excess TG and cholesterol in ob/ob plasma was predominantly found in VLDL-sized fractions upon FPLC separation (data not shown). Liver weight (2-fold), hepatic TG (5-fold), total cholesterol (~2.6-fold), free cholesterol (~1.6-fold), cholesteryl ester (~15-fold) and glycogen levels (~1.8-fold) were all increased in ob/ob mice. No differences in hepatic phospholipid and glucose-6-phosphate (G6P) levels were detected between lean and ob/ob mice (Table 2).

Neutral fat deposition (not shown in figure) in ob/ob mice was clearly associated with the perivenous (zone 3) area of liver lobules resulting in enlarged hepatocytes in these parts of the liver (Figure 1, A vs. B). To check whether localization of fat in ob/ob liver was compatible with that of apolipoprotein B gene expression, *Apob* mRNA was visualized by *in situ* hybridization in lean and ob/ob mouse liver (Figure 1, C and D, respectively). *Apob* mRNA was present in the entire liver lobe but a stronger signal was observed in the periportal zone of the liver both in lean and ob/ob mice, suggesting zonal differentiation between VLDL formation and TG deposition in ob/ob mouse liver.

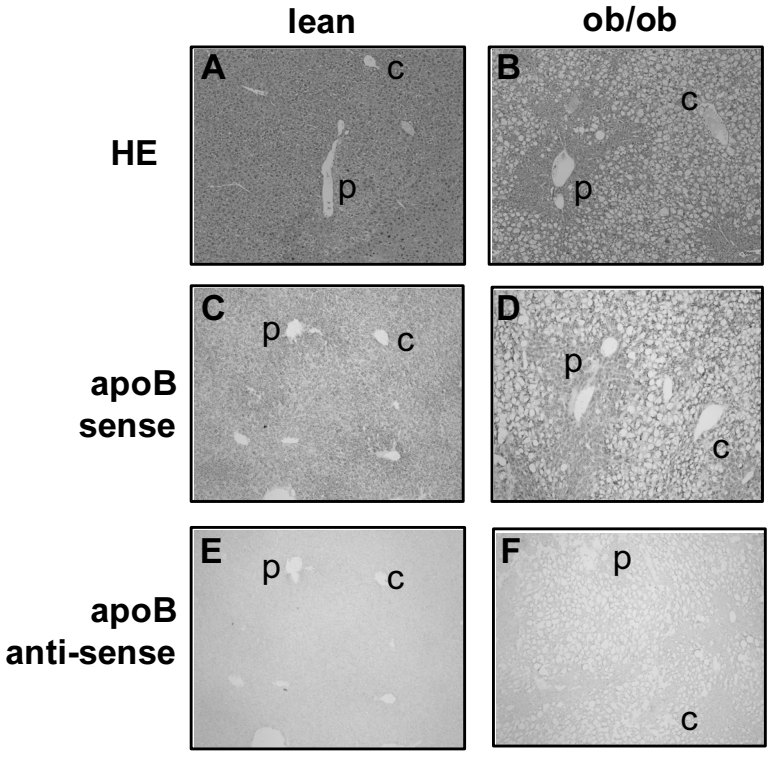

Figure 1. Hematoxilin Eosin (HE) staining (A,B) and apoB *in situ* hybridization (C-F) in liver slides from lean and ob/ob mice, respectively, p=portal area (zone 1), c=central area (zone 3).

***De novo* lipogenesis and cholesterol synthesis.** Palmitate and cholesterol synthesis rates in lean and ob/ob mice fed a [1-^{13}C]-acetate-enriched diet are summarized in Table 3. The enrichment of acetylCoA pool and fractional synthesis rate values could not be calculated in adipose tissue of ob/ob mice due to low isotopic enrichments. Enrichments of the hepatic actylCoA pools for DNL and cholesterogenesis were similar and not different between lean and ob/ob mice. Hepatic fractional *de novo* lipogenesis (DNL) was increased 1.7-fold in ob/ob mice in comparison with lean controls. The absolute amount of newly synthesized hepatic palmitate was 10-fold higher in livers of ob/ob mice than in those from controls. DNL could not be quantified in adipose tissue from ob/ob mice: values in lean controls indicate that adipocytes may significantly contribute to total DNL.

The fractional hepatic cholesterol synthesis was decreased ~1.4 fold in ob/ob mice compared to lean mice. Values for hepatic free cholesterol contents from Table 2 were used to calculate the total amount of newly synthesized cholesterol present in the liver, which was similar in lean and ob/ob mice (Table 3).

To understand the molecular basis of the differences in hepatic lipid synthesis and contents between lean and ob/ob mice, expression levels of relevant genes were determined. Expression levels of key genes involved in FA synthesis, i.e. fatty acid synthase (*Fas*), and acylCoA carboxylase (*Acc*) were clearly increased in livers of ob/ob mice. The mRNA levels for the transcription factor sterol regulatory element binding protein-1c (*Srebp-1c*) was also increased, but gene expression of liver X receptor (*Lxr*) and carbohydrate responsive element-binding protein (*Chrebp*), also implicated in control of *Fas* expression, were significantly decreased. Expression level of the sterol regulatory binding element protein-2 (*Srebp-2*), the transcription factor mainly involved in control of cholesterol synthesis, was decreased in ob/ob mice liver but this did not result in reduced expression of its target gene HMGCoA reductase (*Hmgr*). Hepatic expression levels of the transcription factor peroxisomal proliferator activated receptor-α (*Ppar-α*) was decreased but the expression level of *Ppar-γ* was increased in ob/ob mouse liver. Genes involved in β-oxidation, that are controlled by PPARα, i.e., mitochondrial HMGCoA-synthase (*Hmgs*), carnitine palmitoyl transferase-1a (*Cpt1a*) and medium chain acyl dehydrogenase (*Mcad*), tended to decrease in ob/ob mice, suggesting a decreased β-oxidation in ob/ob mouse liver (Figure 2B).

Table 3. Acetyl CoA pool enrichment and fractional palmitate synthesis values of adipose tissue and liver (A) and hepatic acetyl CoA pool enrichment and fractional cholesterol synthesis values (B) in [1-^{13}C]-acetate-enriched diet fed lean and ob/ob mice (n=5/5), *p<0.05, Mann-Whitney U test, nd = not detectable.

A ***de novo* lipogenesis**	**lean**	**ob/ob**
Liver		
Acetyl CoA pool enrichment (%)	6.3 ± 0.3	5.9 ± 0.8
f liver palmitate (%)	31.0 ± 6.1	53.1± 4.7*
Hepatic palmitate (μmol/liver)	1.1 ± 0.4	6.3 ± 0.9*
Newly synthesized hepatic palmitate (μmol/liver)	0.3 ± 0.1	3.4 ± 0.6*
Adipose tissue		
Acetyl CoA pool enrichment (%)	1.6 ± 0.5	nd
f adipose tissue palmitate (%)	21.5 ± 8.7	nd
B Cholesterol synthesis	**lean**	**ob/ob**
Acetyl CoA pool enrichment (%)	6.3 ± 0.1	5.5 ± 0.5
f hepatic free cholesterol (%)	17.8 ± 4.0	12.6 ± 3.4*
Hepatic free cholesterol (μmol/liver)	1.7 ± 0.1	2.7 ± 0.5*
Newly synthesized hepatic cholesterol (μmol/liver)	0.3 ± 0.1	0.3 ± 0.2

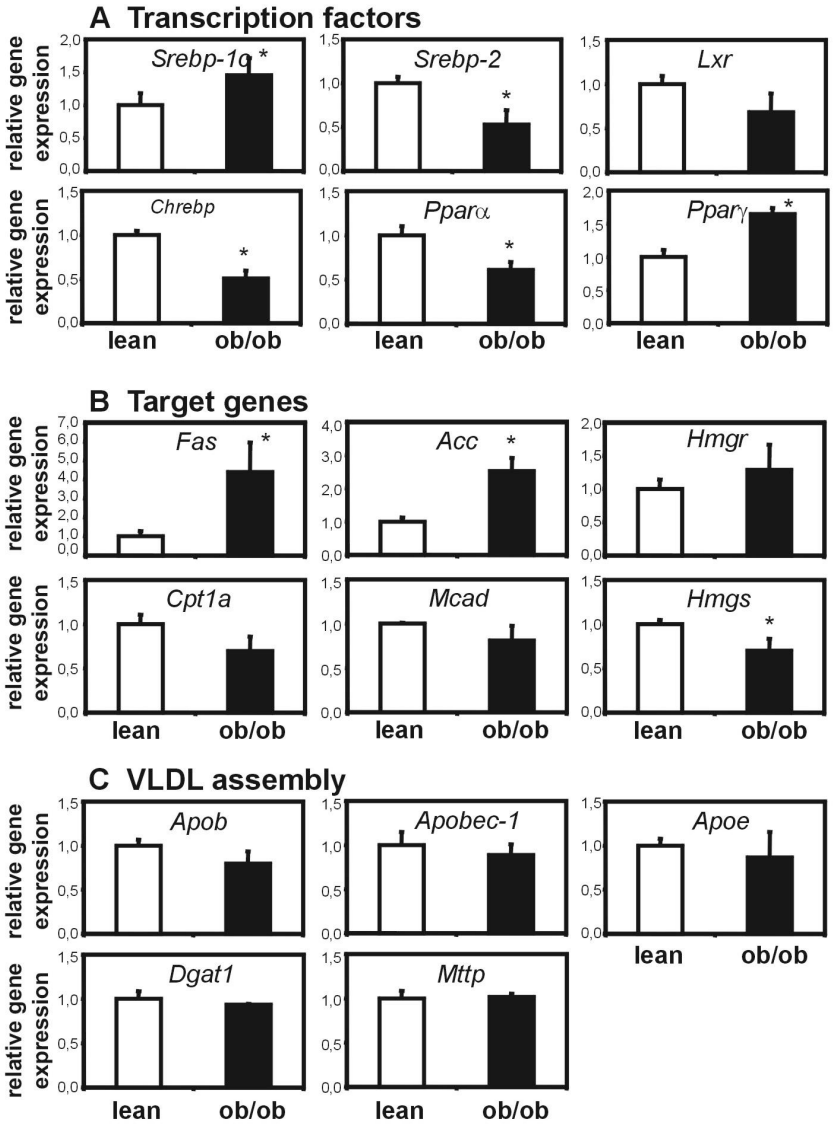

Figure 2. Relative hepatic expression levels of several transcription factors (A), their target genes in fatty acid synthesis, cholesterol synthesis and fatty acid oxidation (B) and genes involved in VLDL assembly (C) in lean (white bars) and ob/ob mice (black bars). Genes are relative to the hepatic β-*Actin* expression level, *p<0.05, Mann-Whitney U test.

Hepatic VLDL production under basal conditions and hyperinsulinemic clamp. VLDL-TG and apoB100 production was measured in anesthetized lean and ob/ob mice during saline infusion (control) and during a hyperinsulinemic clamp. During the hyperinsulinemic clamp, plasma glucose levels were clamped at basal, fasting (9 hr) plasma concentrations and were reached within 60 minutes. Average plasma glucose levels were 7±1 mM and 15±1 mM for lean and ob/ob mice, respectively (Figure 3A). Plasma insulin increased to stable levels of 34±3 ng/ml and 34±2 ng/ml in lean and ob/ob mice, respectively (Figure 3B). Saline infused mice maintained their fasting insulin level during the clamp (0.7±0.4 ng/ml and 5±2 ng/ml in lean and ob/ob mice, respectively). Plasma FFA levels decreased in the insulin-infused mice only (Figure 3C). Although ob/ob mice have higher basal plasma FFA concentrations, insulin reduced plasma FFA levels to the same concentration within 60 minutes as in lean mice.

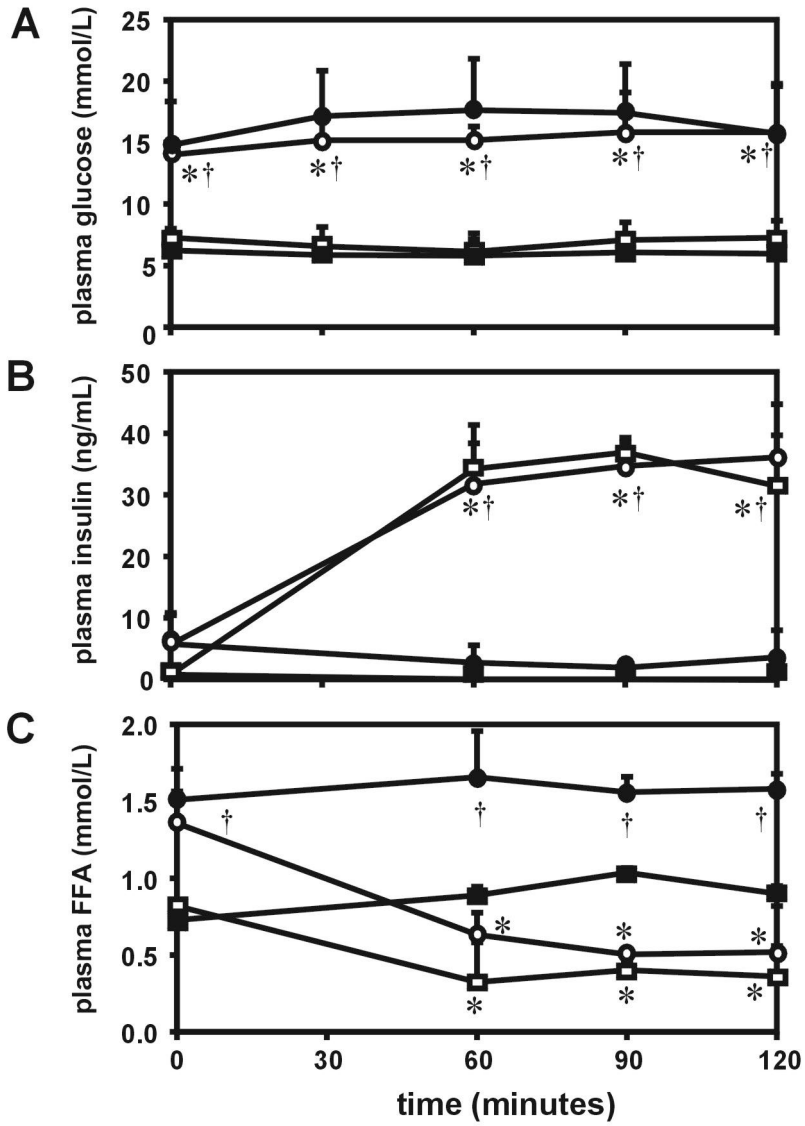

Figure 3. Plasma glucose (A), insulin (B), and FFA (C) levels during a hyperinsulinemic clamp in lean mice receiving saline (closed squares) or insulin (open squares) and in ob/ob mice receiving saline (closed circles) or insulin (open circles). *$p<0.05$ insulin effect, †$p< 0.05$ mouse strain effect, Mann Whitney-U.

After 60 minutes of saline infusion or hyperinsulinemia, Triton WR1339 was injected to determine VLDL-TG and apoB100 production rates. Basal VLDL-TG production rates were similar in lean and ob/ob mice (64±14 and 52±7 μmol/kg/hr, respectively, Figure 4A). Acute hyperinsulinemia reduced VLDL-TG production rate to 27±1 μmol/kg/hr (-58%) in lean mice but only to 41±1 μmol/kg/hr (-21%) in ob/ob mice (Figure 4A). ApoB100 production determined by Western blotting procedure showed a similar pattern as VLDL-TG production rates during the insulin clamp. Insulin suppressed apoB100 production much more pronounced in lean mice than in ob/ob mice (Figure 4B). The apoB100/B48 ratio in nascent VLDL particles, as determined by intensity scanning of Western blots, was much higher in ob/ob mice than in lean controls: this ratio was decreased by insulin infusion.

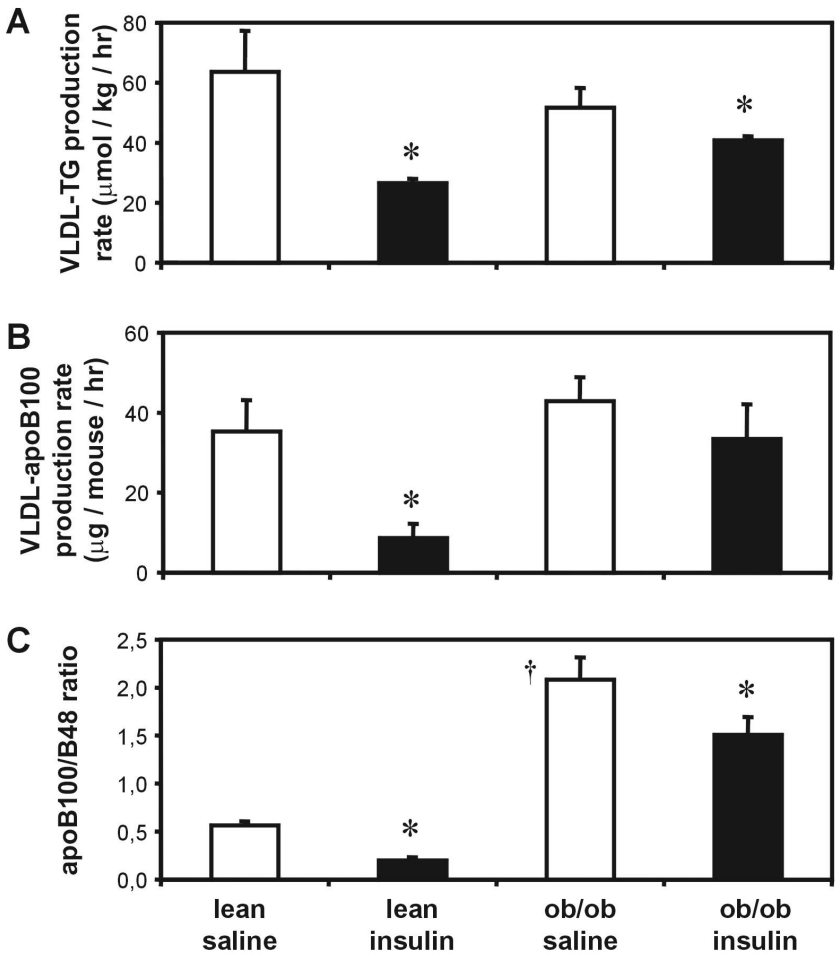

Figure 4. VLDL-TG production rate (A), apoB100 production rate (B), apoB100/B48 band-density-scan-ratio (C) during a hyperinsulinemic clamp in lean and ob/ob mice receiving saline (white bars) or insulin (black bars), n=4/group, *p<0.05 insulin effect, †p<0.05 mouse strain effect, Mann-Whitney U test.

Expression of genes encoding structural proteins of VLDL particles, i.e., apoB and apoE, was similar in liver of lean and ob/ob mice. In spite of the increased apoB100/B48 ratio in ob/ob VLDL, expression of apobec-1, encoding the *Apob* mRNA-editing protein, was not different between both groups indicating a posttranscriptional upregulation of editing activity in ob/ob mice. Expression of the genes encoding MTP and DGAT, enzymes essential for VLDL lipidation, did not differ between lean and ob/ob mice (Figure 2C).

Insulin signaling. Hepatic gene expression levels of the insulin receptor (*Ir*) and insulin receptor substrate isoforms (*Irs1* and *Irs2*) were decreased in ob/ob mice (Figure 5A). Also, phosphorylation of IRβ, IRS-1 and IRS-2 proteins was reduced in ob/ob mice liver (Figure 5B), indicating decreased hepatic insulin signaling. IRS-3 phosphorylation was slightly increased in ob/ob mice liver (Figure 5B).

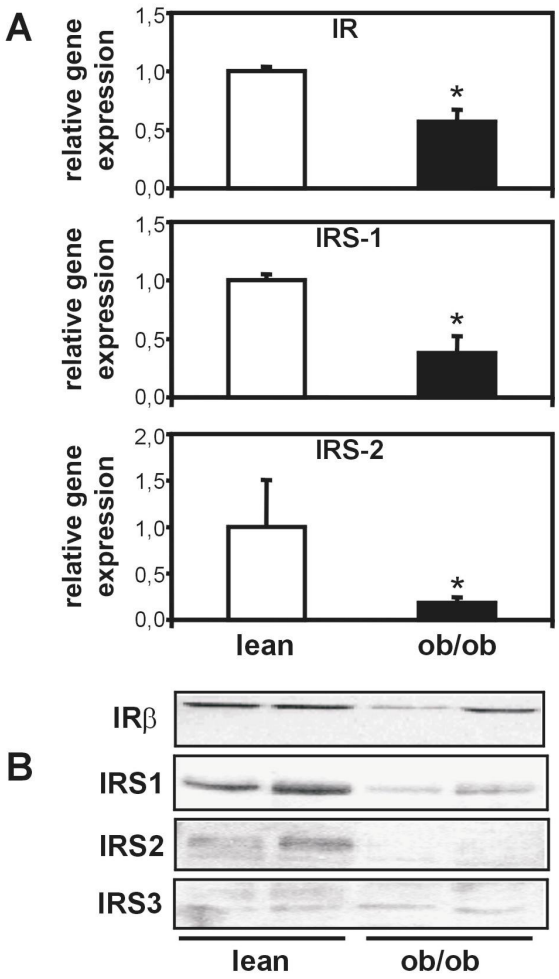

Figure 5. Hepatic gene expression levels (A) and phosphorylation (B) of the insulin receptor (IR) and its substratesIRS-1, -2 and -3 in lean and ob/ob mouse liver, * $p<0.05$, Mann-Whitney U test.

DISCUSSION

The primary defect in the ob/ob mouse model is the absence of leptin, resulting in an obese and diabetic phenotype (5). Ob/ob mice have increased plasma FFA levels, a 10-fold increase in hepatic *de novo* lipogenesis (DNL) and a severe, perivenous localized, hepatic steatosis. Despite these diabetic characteristics, hepatic VLDL production was not increased, as is the case in humans with insulin resistance. We propose that absence of a simultaneous appropriate upregulation of hepatic cholesterol synthesis, recognized as a crucial factor in control of VLDL production rates (32-35) contributes to this discordant phenotype. We further demonstrated that the VLDL production process in ob/ob mice was insensitive to the suppressive effects of insulin, as previously reported in human (2,13) and rodent (36) insulin resistant conditions. This is likely the result of a decrease in the transduction pathway of insulin: in livers of ob/ob mice IRβ, IRS-1 and IRS-2 gene expression levels and protein phosphorylation were clearly decreased. Similar decreases of hepatic and muscle IRS phosphorylation after insulin stimulation *in vivo* were observed in other studies (37-40).

We found DNL, suggested to be a regulator of VLDL production, to be 10-fold

increased in ob/ob liver using MIDA approach. The increase in DNL is probably related to dysregulation of transcriptional control of this pathway due to leptin-deficiency. Expression of enzymes involved in the lipogenesis is under control of at least three transcription factors, i.e., SREBP-1c, LXR and CHREBP (41-43). Interestingly, hepatic SREBP-1c expression levels were increased in ob/ob mice, whereas LXR and CHREBP expression levels were decreased, indicating that SREBP-1c is independently able to strongly induce DNL. SREBP-1c expression is influenced by insulin (44,45). Insulin levels are elevated in ob/ob mouse and may continuously induce expression of SREBP-1c and, thereby, of its target genes (41). Thus, insulin resistance may not involve all branches of insulin signaling. Alternatively, leptin has been shown to be able to downregulate SREBP-1c expression and protein levels and expression of its target gene (*Fas*) in ob/ob adipocytes (46) and in wildtype mouse liver (47). $IRS2^{-/-}$ mice, like ob/ob mice, have increased hepatic SREBP-1c levels, which normalize upon leptin treatment (48). Irrespective of the underlying mechanism, however, our results indicate that upregulated DNL *per se* is not a regulator of hepatic VLDL production by mouse liver.

Theoretically, it may be that TG and apoB, required for VLDL assembly, are functionally separated in the ob/ob liver. Using *in situ* hybridization, we found that *Apob* mRNA is present in all cells in the liver lobule, but with highest intensity in periportal hepatocytes of control mice. Funahashi *et al.* (49) reported a uniform distribution of *Apob* mRNA in rat liver, suggesting the existence of species-differences in this respect. In any case, our results suggest that perivenously localized TG may be less available for VLDL production.

VLDL production in ob/ob mice has been reported to be decreased (15,16) and increased (17) in comparison of that in lean controls. In this study, we found a moderate, not statistically significant decrease in VLDL-TG production in female ob/ob mice under basal conditions (Figure 4A). Although basal production rates for VLDL-TG and -apoB100 were similar in ob/ob and lean mice, acute hyperinsulinemia did not decrease these production rates to the same extent in both genotypes. The insulin-insensitivity in ob/ob mice may lead to a relative overproduction of VLDL particles in postprandial conditions and hence contribute to the hypertriglyceridemia seen in these mice.

In our clamp experiments plasma insulin levels were similar between both groups. However, both groups were clamped at their basal glucose levels resulting in higher glucose levels in ob/ob mice. The question arises to which extent this may have influenced our results with respect to insulin sensitivity of VLDL-TG production. For instance, it may be argued that hyperglycemia in the presence of hyperinsulinemia may stimulate DNL further. This effect might counteract the inhibitory effects of insulin on VLDL-TG secretion. However, in the basal state VLDL production was not increased despite hyperglycemia and a manyfold increase in DNL in ob/ob mice, indicating that this was not a driving force for VLDL secretion. Therefore, it is rather unlikely that hyperglycemia per se the profound insulin resistance with respect to the suppressive effects on VLDL production.

Substrate availability has been proposed to regulate hepatic VLDL output (32,35). Since the availability of plasma FFA, *de novo* synthesized FA and hepatic TG were all increased in ob/ob mice, it is unlikely that the supply of TG is rate-controlling in this respect. In addition, the availability of newly synthesized cholesterol may influence VLDL formation, as has been shown in rats (32), pigs (33), rabbits (34) and in humans treated with cholesterol synthesis inhibitors (35). Total hepatic cholesterol content in ob/ob mouse liver was increased but the absolute cholesterol synthesis rate, as determined by MIDA, was not different compared to lean mice. The transcription factor that is in control of cholesterol synthesis is the sterol regulatory element binding protein-2 (SREBP-2). Sterol regulation is the primary mechanism that dominates cleavage of intracellular, membrane-bound SREBP-2, allowing entry of the active transcription factor into the nucleus to induce expression levels of genes

involved in cholesterol synthesis and uptake. Increased hepatic cholesterol levels were associated with a decreased expression level of SREBP-2 in ob/ob mice, however, this decrease in SREBP-2 expression did not decrease the expression levels of its target gene HMGCoA reductase (Figure 2) nor the absolute cholesterol synthesis rate (Table 3). We hypothesize that limited availability of newly synthesized cholesterol reduces the ability of the liver to remove excess TG as VLDL.

In conclusion, hepatic cholesterol synthesis is not affected but DNL is clearly increased in ob/ob mice, probably related to increased SREBP-1c expression levels and despite downregulation of LXR and CHREBP expression. Insufficient supply of newly synthesized cholesterol may become rate-controlling for VLDL production in ob/ob mice in a situation in which the supply of FA from plasma and DNL is excessive. Metabolic zonation of TG accumulation and apoB production may contribute in this respect. The inability to induce VLDL-production under these conditions, in combination with impaired hepatic β-oxidation, contributes to development of hepatic steatosis, which in itself may contribute to development of hepatic insulin resistance. Hepatic insulin signaling is clearly impaired in ob/ob mice resulting in a decreased ability of insulin to suppress VLDL production.

ACKNOWLEDGMENTS

This work was supported by the Netherlands Diabetes Foundation (grant 96.604). We thank Vincent Bloks and Juul Baller for their excellent technical assistance.

REFERENCES

1. Nestel,P, Goldrick,B: Obesity: changes in lipid metabolism and the role of insulin. *Clin Endocrinol Metab* 5:313-335, 1976
2. Kissebah,AH, Alfarsi,S, Evans,DJ, Adams,PW: Integrated regulation of very low density lipoprotein triglyceride and apolipoprotein-B kinetics in non-insulin-dependent diabetes mellitus. *Diabetes* 31:217-225, 1982
3. Jungermann,K, Kietzmann,T: Oxygen: Modulator of metabolic zonation and disease of the liver. *Hepatology* 31:255-260, 2000
4. Guzman,M, Castro,J: Zonation of fatty acid metabolism in rat liver. *Biochem.J* 264:107-113, 1989
5. Picard,F, Richard,D, Huang,Q, Deshaies,Y: Effects of leptin adipose tissue lipoprotein lipase in the obese ob/ob mouse. *Int J Obes Relat Metab Disord* 22:1088-1095, 1998
6. Shimomura,I, Bashmakov,Y, Horton,JD: Increased levels of nuclear SREBP-1c associated with fatty livers in two mouse models of diabetes mellitus. *J Biol Chem* 274:30028-30032, 1999
7. Levin,N, Nelson,C, Gurney,A, Vandlen,R, Sauvage de,F: Decreased food intake does not completely account for adiposity reduction after ob protein infusion. *PNAS* 93:1726-1730, 1996
8. Hron,WT, Sobocinski,KA, Menahan,LA: Enzyme activities of hepatic glucose utilization in the fed and fasting genetically obese mouse at 4-5 moths of age. *Horm Metab Res Suppl* 16:32-36, 1984
9. Reul,BA, Becker,DJ, Ongemba,LN, Bailey,CJ, Henquin,JC, Brichard,SM: Improvement of glucose homeostasis and hepatic insulin resistance in ob/ob mice given oral molybdate. *J Endocrinol* 155:55-64, 1997
10. Yen,TT, Allan,JA, Yu,PL, Acton,MA, Pearson,DV: Triacylglycerol contents and in vivo lipogenesis of ob/ob, db/db and Avy/a mice. *Biochim Biophys Acta* 441:213-220, 1976
11. Memon,RA, Fuller,J, Moser,AH, Smith,PJ, Grunfeld,C, Feingold,KR: Regulation of putative fatty acid transporters and acyl-CoA synthetase in liver and adipose tissue in *ob/ob* mice. *Diabetes* 48:121-127, 1999

12. Nikkila,EA, Kekki,M: Plasma triglyceride transport kinetics in diabetes mellitus. *Metabolism* 22:1-22, 1973
13. Lewis,GF, Uffelman,KD, Szeto,LW, Steiner,G: Effects of acute hyperinsulinemia on VLDL triglyceride and VLDL apoB production in normal weight and obese individuals. *Diabetes* 42:833-842, 1993
14. Malmstrom,R, Packard,CJ, Watson,TD, Rannikko,S, Caslake,M, Bedford,D, Stewart,P, Yki-Jarvinen,H, Shepherd,J, Taskinen,MR: Metabolic basis of hypotriglyceridemic effects of insulin in normal men. *Arterioscler Thromb Vasc Biol* 17:1454-1465, 1997
15. Li,X, Grundy,SM, Patel,SB: Obesity in *db* and *ob* animals leads to impaired hepatic very low density lipoprotein secretion and differential secretion of apolipoprotein B-48 and B-100. *J Lip Res* 38:1277-1288, 1999
16. Camus,MC, Aubert,R, Bourgeois,F, Herzog,J, Alexiu,A, Lemonnier,D: Serum lipoprotein and apolipoprotein profiles of the genetically obese ob/ob mouse. *Biochim Biophys Acta* 961:53-64, 1988
17. Bartels,ED, Lauritsen,M, Nielsen,LB: Hepatic expression of microsomal triglyceride transfer protein and in vivo secretion of triglyceride-rich lipoproteins are increased in obese diabetic mice. *Diabetes* 51:1233-1239, 2002
18. Hawkins,M, Barzilai,N, Liu,R, Chen,W, Rossetti,L: Role of glucosamine pathway in fat-induced insulin resistance. *J Clin Invest* 99:2173-2182, 1997
19. Rossetti,L, Barzilai,N, Chen,W, Harris,T, Yang,D, Rogler,CE: Hepatic overexpression of insulin-like growth factor-II in adulthood increases basal and insulin-stimulated glucose disposal in conscious mice. *J Biol Chem* 271:203-208, 1996
20. Li,X, Catalina,F, Grundy,SM, Patel,S: Method to measure apolipoprotein B-48 and B-100 secretion rates in an individual mouse: evidense for a very rapid turnover of VLDL and preferential removal of B-48 relative to B-100-containing lipoproteins. *J Lip Res* 37:210-220, 1996
21. Bligh,EG, Dyer,WJ: A rapid metod of total lipid extraction and purification. *Can J Biochem Physiol* 37:911-917, 1959
22. Lowry,OH, Rosebrough,NJ, Farr,AL, Randall,RL: Protein measurement with the folin reagens. *J Biol Chem* 193:265-275, 1951
23. Mensenkamp,AR, Teusink,B, Baller,JF, Wolters,H, Havinga,R, Van Dijk,KW, Havekes,LM, Kuipers,F: Mice expressing only the mutant APOE3Leiden gene show impaired VLDL secretion. *Arterioscler Thromb Vasc Biol* 21:1366-1372, 2001
24. Hellerstein,MK, Neese,RA: Mass isotopomer distribution analysis: a technique for measuring biosynthesis and turnover of polymers. *Am J Physiol* 263:E988-E1001, 1992
25. Hellerstein,MK, Neese,RA: Mass isotopomer distribution analysis at eight years: heoretical, analysis, and experimental considerations. *Am J Physiol* 276:E1146-E1170, 1999
26. Neese,RA, Faix,D, Kletke,C, Wu,K, Wang,AC, Shackleton,CH, Hellerstein,MK: Measurement of endogenous synthesis of plasma cholesterol in rats and humans using MIDA. *Am J Physiol* 264:E136-E147, 1993
27. Lepage,G, Roy,CC: Direct transesterification of all classes of lipids in a one-step reaction. *J Lipid Res* 27:114-120, 1986
28. Minich,DM, Kalivianakis,M, Havinga,R, van Goor,H, Stellaard,F, Vonk,RJ, Kuipers,F, Verkade,HJ: Bile diversion in rats leads to a decreased plasma concentration of linoleic acid which is not due to decreased net intestinal absorption of dietary linoleic acid. *Biochim Biophys Acta* 1438:111-119, 1999
29. Curtin,A, Deegan,P, Owens,D, Collins,P, Johnson,A, Tomkin,GH: Elevated triglyceride-rich lipoproteins in diabetes. A study of apolipoprotein B-48. *Acta Diabetol* 33:205-210, 1996
30. Ouwens,DM, van der Zon,GC, Pronk,GJ, Bos,JL, Moller,W, Cheatham,B, Kahn,CR, Maassen,JA: A mutant insulin receptor induces formation of a Shc-growth factor receptor bound protein 2 (Grb2) complex and p21ras-GTP without detectable interaction of insulin receptor substrate 1 (IRS1) with Grb2. Evidence for IRS1-independent p21ras-GTP formation. *J Biol Chem* 269:33116-33122, 1994
31. Telting,D, van der Zon,GC, Dorrestijn,J, Maassen,JA: IRS-1 tyrosine phosphorylation reflects insulin-induced metabolic and mitogenic responses in 3T3-L1 pre-adipocytes. *Arch Physiol Biochem* 109:52-62, 2001

32. Khan,B, Wilcox,HG, Heimberg,M: Cholesterol is required for secretion of very-low-density lipoprotein by rat liver. *Biochem J* 258:807-816, 1989
33. Burnett,JR, Wilcox,LJ, Telford,DE, Kleinstiver,SJ, Barrett,PH, Newton,RS, Huff,MW: Inhibition of ACAT by avasimibe decreases both VLDL and LDL apolipoprotein B production in miniature pigs. *J Lipid Res* 40:1317-1328, 1999
34. Mackinnon,AM, Savage,J, Gibson,RA, Barter,PJ: Secretion of cholesteryl ester-enriched very low density lipoproteins by the liver of cholesterol-fed rabbits. *Atherosclerosis* 54:145-155, 1985
35. Watts,GF, Naoumova,R, Cummings,MH, Umpleby,AM, Slavin,BM, Sonksen,PH, Thompson,GR: Direct correlation between cholesterol synthesis and hepatic secretion of apolipoprotein B-100 in normolipidemic subjects. *Metabolism* 44:1052-1057, 1995
36. Wiegman,CH, Ouwens,DM, Havinga,R, van der Sluijs,FH, Meijer,AJ, Sauerwein,HP, Romijn,JA, Kuipers,F: Dietary fat-induced hepatic insulin resistance with regard to VLDL prodution in rats. *submitted manuscript* 2002
37. Folli,F, Saad,MJA, Backer,JM, Kahn,CR: Regulation of phosphatidylinositol 3-kinase activity in liver and muscle of animal models of insulin-resistant and insulin-deficient diabetes mellitus. *J Clin Invest* 92:1787-1794, 1993
38. Saad,MJA, Araki,E, Miralpeix,M, Rothenberg,PL, White,MF, Kahn,CR: Regulation of insulin receptor substrate-1 in liver and muscle of animal models of insulin resistance. *J Clin Invest* 90:1839-1849, 1992
39. Kerouz,NJ, Horsch,D, Pons,S, Kahn,CR: Differential regulation of insulin receptor substrates-1 and -2 (IRS-1 and IRS-2) and phosphatidylinositol 3-kinase isoforms in liver and muscle of the obese diabetic (ob/ob) mouse. *J Clin Invest* 100:3164-3172, 1997
40. Shimomura,I, Matsuda,M, Hammer,RE, Bashmakov,Y, Brown,MS, Goldstein,JL: Decreased IRS-2 and increased SREBP-1c lead to mixed insulin resistance and sensitivity in livers of lipodystrophic and ob/ob mice. *Mol Cell* 6:77-86, 2000
41. Koo,S-H, Dutcher,AK, Towle,HC: Glucose and insulin function through two distinct transcription factors to stimulate expression of lipogenic enzyme genes in liver. *J Biol Chem* 276:9437-9445, 2001
42. Yamashita,H, Takenoshita,M, Sakurai,M, Bruick,RK, Henzel,WJ, Shillinglaw,W, Arnot,D, Uyeda,K: A glucose-responsive transcription factor that regulates carbohydrate metabolism in the liver. *PNAS* 98:9116-9121, 2001
43. Kawaguchi,T, Osatomi,K, Yamashita,H, Kabashima,T, Uyeda,K: Mechanism for fatty acid "sparing" effect on glucose-induced transcription: regulation of carbohydrate-responsive element-binding protein by AMP-activated protein kinase. *J Biol Chem* 277:3829-3835, 2002
44. Foretz,M, Guichard,C, Ferre,P, Foufelle,F: Sterol regulatory element binding protein-1c is a major mediator of insulin action on the hepatic expression of glucokinase and lipogenesis-related genes. *PNAS* 96:12737-12742, 1999
45. Kim,JB, Sarraf,P, Wright,M, Yao,KM, Mueller,E, Solanes,G, Lowell,BB, Spiegelman,BM: Nutritional and insulin regulation of fatty acid synthetase and leptin gene expression through ADD1/SREBP1. *J Clin Invest* 101:1-9, 1998
46. Soukas,A, Cohen,P, Socci,ND, Friedman,JM: Leptin-specific patterns of gene expression in white adipose tissue. *Genes Dev* 14:963-980, 2000
47. Kakuma,T, Lee,Y, Higa,M, Wang,Z-W, Pan,W, Shimomura,I, Unger,RH: Leptin, troglitazone, and the expression of sterol regulatory element binding proteins in liver and pancreatic islets. *PNAS* 97:8536-8541, 2000
48. Tobe,K, Suzuki,R, Aoyama,M, Yamauchi,T, Kamon,J, Kubota,N, Terauchi,Y, Matsui,J, Akanuma,Y, Kimura,S, Tanaka,J, Abe,M, Ohsumi,J, Nagai,R, Kadowaki,T: Increased expression of the sterol regulatory element binding protein-1 gene in insulin receptor substrate-2 (-/-) mouse liver. *J Biol Chem* 276:38337-38340, 2001
49. Funahashi,T, Giannoni,F, DePaoli,AM, Skarosi,SF, Davidson,NO: Tissue-specific, developmental and nutritional regulation of the gene encoding the catalytic subunit of the rat apolipoprotein B mRNA editing enzyme: functional role in the modulation of apoB mRNA editing. *J Lipid Res* 36:414-428, 1995